413

Estimating Erosion and Sediment Yield on Field-Sized Areas

G. R. Foster, L. J. Lane, J. D. Nowlin, J. M. Laflen, R. A. Young
MEMBER ASAE · MEMBER ASAE · MEMBER ASAE

ABSTRACT

A model for field-sized areas was developed to evaluate sediment yield under various management practices. The model provides a tool for evaluating sediment yield on a storm-by-storm basis for control of erosion and sediment yield from farm fields. The model incorporates fundamental principles of erosion, deposition, and sediment transport. The procedures allow parameter values to change along complex overland flow profiles and along waterways to represent both spatial variability and variations that occur from storm to storm. Many of the model parameter values are obtained from topographic maps or directly from the Universal Soil-Loss Equation (USLE). Thus we feel that the model has immediate applications without extensive calibration.

Individual components of the model were tested using experimental data from studies of overland flow, erodible channels, and small impoundments. These results suggest that the model produces reasonable estimates of erosion, sediment transport, and deposition under a variety of conditions common to field-sized areas. The procedures developed here can be used to evaluate alternative management practices such as conservation tillage, terracing, and contouring.

INTRODUCTION

Estimates of erosion and sediment yield on field-sized areas are needed so that best management practices (BMPs) can be selected to control erosion for maintaining soil productivity and to control sediment yield for preventing excessive degradation of water quality. The field is typically the management unit used by most farmers to select management practices. For several years, soil conservationists have used the Universal Soil-Loss Equation (USLE) (Wischmeier and Smith, 1978) to select erosion control practices tailored for a given farmer and his fields. If sediment yield tolerances for maintenance of water quality are established for local areas, a model is needed to select BMPs based on a farmer's site specific conditions, his needs, and tolerable loading rates for streams in his area.

On a given field, sediment yield is controlled by either sediment detachment or sediment transport capacity (Ellison, 1947; Meyer and Wischmeier, 1969), depending on factors such as topography, soil, cover, and rainfall/runoff characteristics. The effects of these factors change from season to season and from storm to storm. The need to consider detachment and transport processes on a storm-by-storm basis limits the accuracy of lumped equations such as the USLE (an erosion equation), or Williams' (1975) modified USLE (a flow transport sediment yield equation) on field-sized areas.

Several detailed models (Beasley et al., 1980; Donigian and Crawford, 1976; Li, 1977) compute erosion and sediment transport at various times over a runoff event. Although these models are powerful, their considerable use of computer time prohibits the practical simulation of long periods of record on many fields to select a BMP for specific fields.

The purpose of this paper is to describe a model that, while simply constructed and usable over a broad range of situations at reasonable cost, embodies the latest knowledge on the fundamentals of erosion mechanics. The model may be used without calibration or collection of data to determine parameter values. It can be linked to hydrologic and chemical transport models, and was developed for that specific purpose as a component of CREAMS, a field scale model for Chemicals, Runoff, and Erosion from Agricultural Management Systems (USDA, 1980).

BASIC CONCEPTS

The basis of this model is that USLE storm erosivity, EI, and the peak runoff rate at the watershed outlet can be used to characterize a storm's rainfall, runoff, and sediment yield. Quasi-steady state is assumed. Thus, sediment movement downslope obeys continuity expressed by:

$$dq_s/dx = D_L + D_F \quad [1]$$

where q_s = sediment load (mass/unit width/unit time), x = distance, D_L = lateral inflow of sediment (mass/unit area/ unit time), and D_F = detachment or deposition by flow (mass/unit area/unit time). Mathematically, detachment and deposition differ only in sign; detachment is positive, deposition is negative.

Hydrologically and hydraulically, a typical watershed may be divided into areas or elements of overland flow, channel flow, or impounded runoff. Each type of flow is

---

Article was submitted for publication in September 1980; reviewed and approved for publication by the Soil and Water Division of ASAE in March 1981.

Contribution from USDA-SEA-AR in cooperation with the Purdue Agricultural Experiment Station, Purdue Journal No. 8111.

The authors are: G. R. FOSTER, Hydraulic Engineer, USDA, and Associate Professor, Agricultural Engineering Dept., Purdue University, Lafayette, IN; L. J. LANE, Hydrologist, USDA, Tucson, AZ; J. D. NOWLIN, Computer Programmer, USDA, Agricultural Engineering Dept., Purdue University, Lafayette, IN; J. M. LAFLEN, Agricultural Engineer, USDA, Ames, IA; and R. A. YOUNG, Agricultural Engineer, USDA, Morris, MN.

Acknowledgements: The erosion-sediment yield model described herein is a component of CREAMS, a comprehensive field-scale model including hydrologic, erosion, pesiticide, and nutrient components developed by USDA-SEA-AR scientists under the leadership of W. G. Knisel, Jr. Complete documentation on the comprehensive model is given by USDA (1980). Additional support for this project, including computer programming by V. A. Ferreira, was provided by K. G. Renard, Research Leader, Southwest Rangeland Watershed Research Center, USDA-SEA-AR, Tucson, AZ; W. C. Moldenhauer, Research Leader, Erosion Research Unit, USDA-SEA-AR, Lafayette, IN; and G. W. Isaacs, Head, Agricultural Engineering Dept., Purdue University, W. Lafayette, IN.

This article is reprinted from the TRANSACTIONS of the ASAE (Vol. 24, No. 5, pp. 1253-1262, 1981)

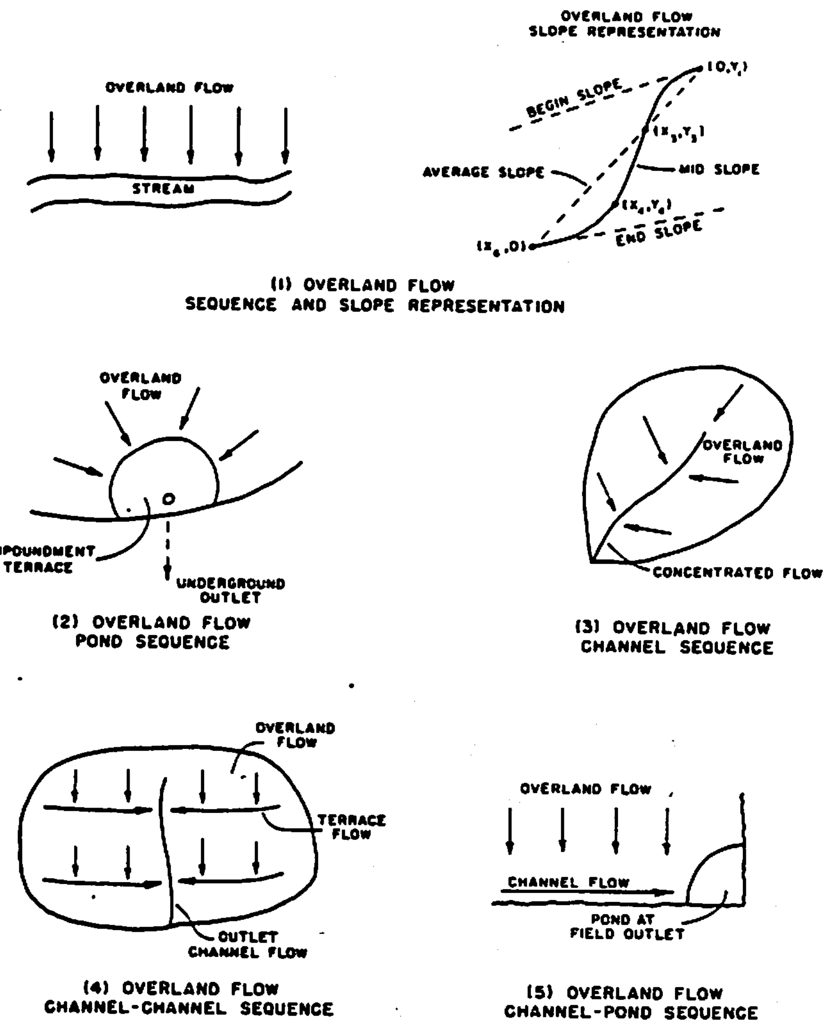

FIG. 1 Schematic representation of typical field systems in the field-scale erosion/sediment yield model.

treated in the model with a specific set of equaions for that type of flow. Lateral sediment inflow is from interrill erosion on overland flow areas, or from overland flow (or channels if a set of channels drain into a main channel) for the channel areas. Overland flow or channels, but not both, may drain directly into an impoundment according to the model's structure. Flow in rills on overland flow areas or in channels transports all sediment downstream. Lateral sediment inflow to runoff in rills or channels is assumed regardless of whether the flow is detaching or depositing.

The watershed is represented by selecting a combination of elements from a typical overland flow profile, a main channel, a set of channels draining into a main channel, or a small impoundment as illustrated in Fig. 1. The selected combination of elements depends on the site being analyzed. Overland flow and channel elements are divided into segments along their length. Computations proceed downstream segment by segment and element by element. The computational sequence is shown in Fig. 2.

For an overland flow or channel segment, the model computes a potential sediment load which is the sum of the sediment load from the immediate upslope segment plus that added by lateral inflow within the segment. If the potential load is less than the sediment transport capacity of the flow, detachment occurs either at the detachment capacity of the flow or at the rate that will just fill transport capacity, whichever is less. Sediment detachment by rainfall or flow adds sediment having a given size and density distribution. No sorting is allowed during detachment.

If potential sediment load is greater than transport capacity, deposition is assumed to occur at the rate of (Foster and Meyer, 1975):

$$D_d = \alpha (T_c - q_s) \quad \text{[2]}$$

where D_d = deposition rate (mass/unit area/unit time), α = a first order reaction coefficient (length $^{-1}$), and T_c = transport capacity (mass/unit width/unit time). The coefficient α is given by:

$$\alpha = \xi V_s / q_w \quad \text{[3]}$$

where ξ = 0.5 for overland flow (Davis, 1978), and 1.0 for channel flow (Einstein, 1968), V_s = particle fall velocity, and q_w = discharge per unit width (volume/unit width/unit time). Fall velocity is computed using standard relationships and drag coefficients for a sphere falling in still water.

The assumption that dT_c/dx is constant over a segment permitted use of analytical solutions to equations [1] and [2] where deposition occurred. Where deposition did not occur, sediment load was calculated from:

$$q_s = (D_u + D_l)\Delta x/2 + D_L \Delta x + q_{su} \quad \text{[4]}$$

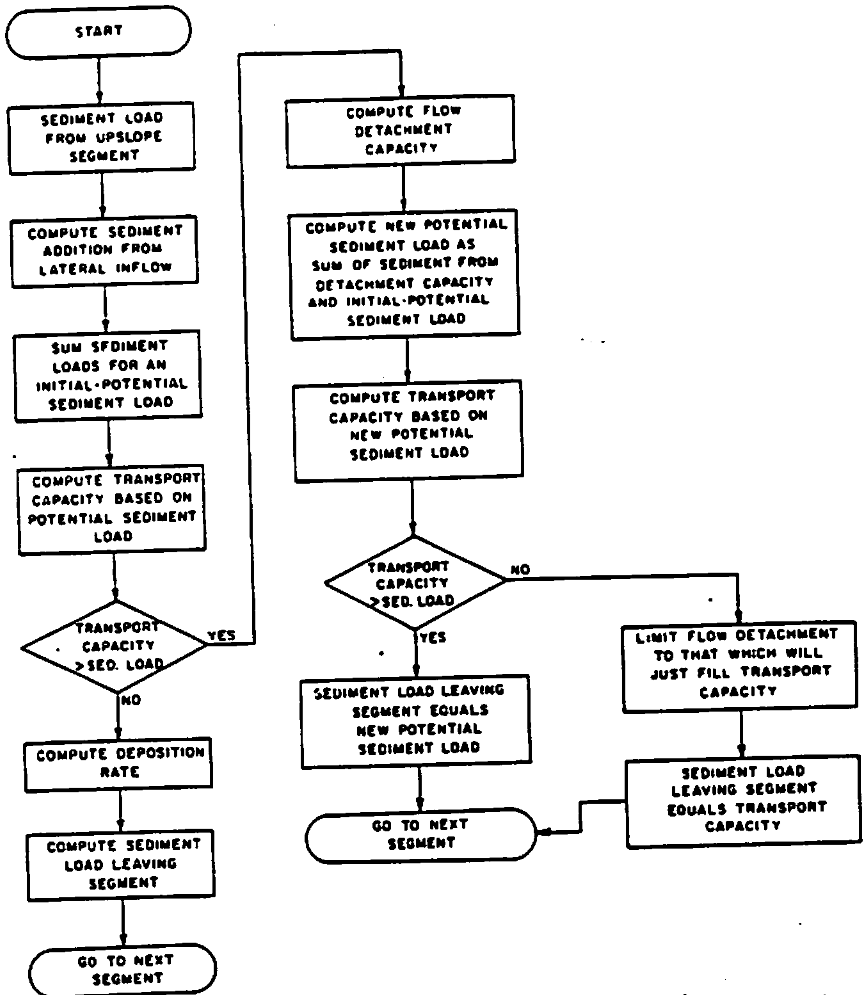

FIG. 2 Flow chart for detachment-transport-deposition computations within a segment of an overland flow or channel element.

where D_u and D_l respectively, rates of detachment by flow at the upper and lower ends of the segment or its portion where detachment by flow is occurring, Δx = length of the segment or its portion where detachment by flow is occurring, and q_{su} = sediment load at the upper end of the segment or its portion where detachment by flow is occurring.

The Yalin sediment transport equation was modified (Yalin, 1963; Foster and Meyer, 1972; Davis, 1978; and Khaleel et al., 1979) to describe sediment transport capacity for various particle sizes and densities. A particle type is a class of particles represented by a given diameter and specific gravity. If transport capacity exceeds availability for one particle type while it is less for another, excess transport capacity is shifted from the particle type having the excess to the one having the deficit. Furthermore, simultaneous deposition and detachment of particles by flow is not allowed. Equations [1 - 4] are solved for each particle type within these constraints.

OVERLAND FLOW ELEMENT

Detachment on interrill and rill areas and transport and deposition by flow in rills are the important erosion-transport processes on overland flow areas. Detachment is described by a modified USLE written as (Foster et al., 1977):

$$D_{Li} = 4.57\ EI\ (s_o + 0.014) K \Phi P\ (\sigma_p / V_u) \quad \ldots\ldots\ldots\ldots [5]$$

and

$$D_{Fr} = (6.86 \times 10^6)\ \eta\ v_u \sigma_p^{1/3}\ (x/22.1)^{\eta - 1} K \Phi P\ (\sigma_p / V_u) \quad \ldots [6]$$

where D_{Li} = interrill detachment rate (g/m² of land surface/s), D_{Fr} = capacity rate for rill detachment (g/m² of land surface/s), EI = rainfall erosivity (energy times maximum 30-min intensity) (N/h)*, x = distance downslope (m), s_o = sine of slope angle, η = slope length exponent for rill erosion, K = USLE soil erodibility factor* [g h/ (N m²)], Φ = USLE cover-management soil-loss ratio, P = USLE contouring factor, V_u = runoff amount [volume/unit area (m)], and σ_p = peak runoff rate [volume/unit area/unit time (m/s)]. The term σ_p/V_u converts a total soil loss for a storm to an average rate for the storm. Only the contouring part of the USLE P factor is used. The model is structured to directly account for other supporting conservation practices like terraces and stripcropping.

For downslope distances less than 50 m, η is set to 2.0, but for slopes longer than 50 m, η is limited by:

$$\eta = 1.0 + 3.912 / \ln x \quad \ldots\ldots\ldots\ldots [7]$$

*The units on the K factor from the USLE must be carefully noted. Multiplication of the K in U. S. customary units by 131.7 gives a metric K having units of gh/(Nm²). Foster, G. R., D. K. McCool, K. G. Renard and W. C. Moldenhauer. 1981. Conversion of the Universal Soil-Loss Equation (USLE) to metric SI units. Accepted by J. Soil and Water Conservation. Manuscript available from senior author.

This limit avoids apparent excessive rill erosion for very long slopes (Foster et al., 1977). Equation [7] limits the effective slope length exponent for rill and interrill erosion combined to 1.67 so far as it is a function of length. The effective exponent is also a function of slope and runoff erosivity relative to rainfall erosivity.

The detachment equations [5] and [6] (except for the σ_p/V_u term) as originally developed (Foster et al., 1977) were on a storm basis, whereas the transport equation is on an instantaneous rate basis. The two were combined by assuming that the computed sediment concentrations are average concentrations for the runoff event.

Cover and management effects on detachment are described with the USLE soil loss ratios (Wischmeier and Smith, 1978). Cover and management affect transport by their reduction of σ_p and V_u (estimated outside of the model) and by reducing the flow's shear stress acting along the soil-water interface. The concept (Graf, 1971) of dividing shear between form roughness (cover like mulch or vegetation) and grain roughness (soil) is used to estimate the proportion of total shear stress acting on the soil. The shear stress acting on the soil, τ_{soil}, is estimated by:

$$\tau_{soil} = \gamma y s_o (n_{bov}/n_{cov})^{9/10} \quad \text{[8]}$$

where Y = weight density of water, y = flow depth for bare, smooth soil, n_{bov} = Manning's n for bare soil, and n_{cov} = Manning's n for rough, mulch, or vegetative covered soil. Flow depth is estimated by the Manning equation as:

$$y = [q_w n_{bov}/s^{1/2}]^{3/5} \quad \text{[9]}$$

where q_w = discharge rate per unit width. Although the Darcy-Weisbach equation with a varying friction factor for laminar flow might be more accurate in some cases for y, most users are better acquainted with estimating Manning's n. Values for Manning's n may be selected from Foster et al. (1980a) and Lane et al. (1975).

Segments along the overland flow profile are established by the model. The overland flow profile may be uniform, convex, concave, or a combination of these shapes. Input data requirements are slope length, average slope steepness, location of the end points of a uniform section at midslope, slope at the upper end of the profile, and slope at the lower end of the profile. A quadratic curve is fitted to curved portions of the slope so that it passes through an end point of the uniform segment at midslope and is tangent to the profile near each of its ends. Convex portions of a profile are divided into three equal length segments while concave portions are divided into ten equal length segments because calculation of deposition on concave slopes is quite sensitive to the number of segments, and accurate computation of the location of the beginning of deposition is important. Uniform portions of a profile are single segments. Additional segment ends are designated by the model where K, Φ, P, or n_{cov} change.

CHANNEL ELEMENT

The channel element describes detachment, transport, and deposition by flow in terrace channels, diversions, natural waterways, grassed waterways, row middles or graded rows, tailwater ditches, and other similar channels where topography has caused overland flow to converge. The channel element does not describe erosion in gullies or large streams.

The same basic concepts are used in both the channel and overland flow elements. Discharge along the channel is assumed to vary directly with upstream drainage area. An initial discharge is permitted at the upper end of a channel to account for upland contributing areas. Changes in controlling variables like slope and cover along the channel are allowed.

Flow in most channels in fields is spatially varied, with discharge increasing along the channel. The model approximates the energy gradeline along the channel assuming a triangular channel section and steady flow at the characteristic peak discharge from a set of polynomial curves fitted to solutions of the normalized spatially varied flow equation (Chow, 1959). This feature approximates either drawdown or backwater at a channel outlet like at the edge of a field where vegetation may hinder runoff. As an alternative in the model, the slope of the energy gradeline can be assumed equal to the channel slope. After the slope of the energy gradeline is estimated, a triangular, rectangular, or "naturally eroded" section is selected at the user's option to compute flow hydraulics and channel erosion and sediment transport.

In the spring immediately after planting, concentrated flow from intense rains on a freshly prepared seedbed may erode through the finely tilled layer to the depth of secondary tillage. If the soil is susceptible to erosion by flow when tilled, the flow may erode deeper to the depth of primary tillage. Often the soil is much less erodible at this level and downcutting will stop here. Before the channel reaches a nonerodible layer, its width is a function of the flow's shear stress and the soil's critical shear stress. Once the flow reaches a relatively nonerodible layer, the channel widens. As it widens, the erosion rate decreases until it approaches zero as the channel approaches a maximum width. The maximum width depends on the flow's shear stress and the soil's critical shear stress. Data from rill erosion studies (Meyer et al., 1975; Lane and Foster, 1980) suggest that erosion by flow over a tilled, loose seedbed may be described by:

$$D_c = K_{ch} (1.35\bar{\tau} - \tau_{cr})^{1.05} \quad \text{[10]}$$

where D_c = erosion rate in a channel (mass/unit area of wetted perimeter/unit time), K_{ch} = soil erodibility factor for a channel erosion $\bar{\tau}$ = average shear of the flow at a channel section, and τ_{cr} = a critical shear stress below which erosion is negligible. Critical shear stress of the surface layer of soil seems to increase greatly over the year as the soil consolidates (Graf, 1971; Foster et al., 1980a).

The shear stress acting on the soil is the shear stress used to compute detachment and sediment transport capacity. Grass and mulch reduce this stress. Total shear is divided into that acting on the vegetation, mulch, or large scale roughness and that acting on the soil using sediment transport theory (Graf, 1971).

Shear stress at a channel location varies with time as runoff rises and falls. The model assumes that shear stress is triangularly distributed in time during the runoff event to estimate the time t_b that shear stress exceeds the critical shear stress. Shear stress is assumed constant and equal to shear stress computed from the characteristic peak discharge for this time period. This tends to overestimate total erosion for the storm. The derivation and

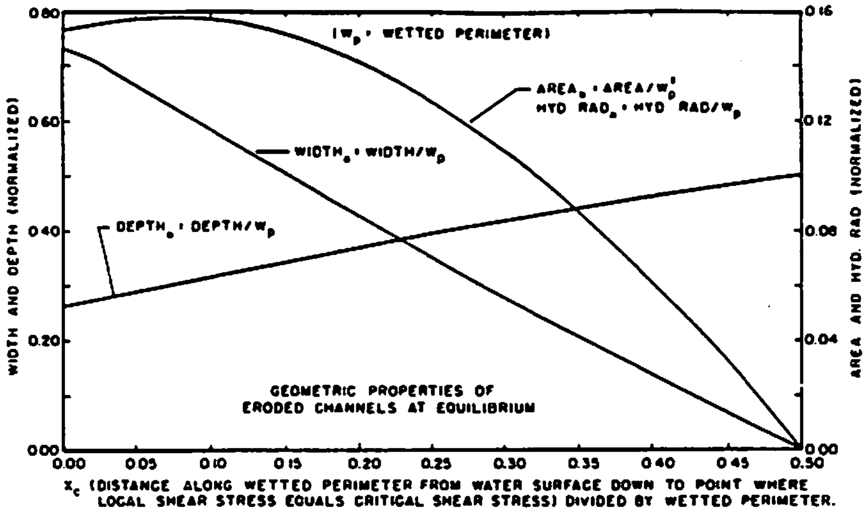

FIG. 3 Geometric properties of an eroding channel at equilibrium.

validation of the equations for channel erosion discussed below were described by Lane and Foster (1980).

Until the channel reaches the nonerodible layer, an active channel is assumed to be rectangular with the width obtained by Fig. 3 and 4 and equations [11] and [12]. The solution requires that a value for x_c be found. Given the discharge Q, Manning's n, and friction slope S_f, a value $g(x_c)$ is calculated from:

$$g(x_c) = (Qn/S_f^{1/2})^{3/8}\ (\gamma S_f/\tau_{cr}) \quad \text{[11]}$$

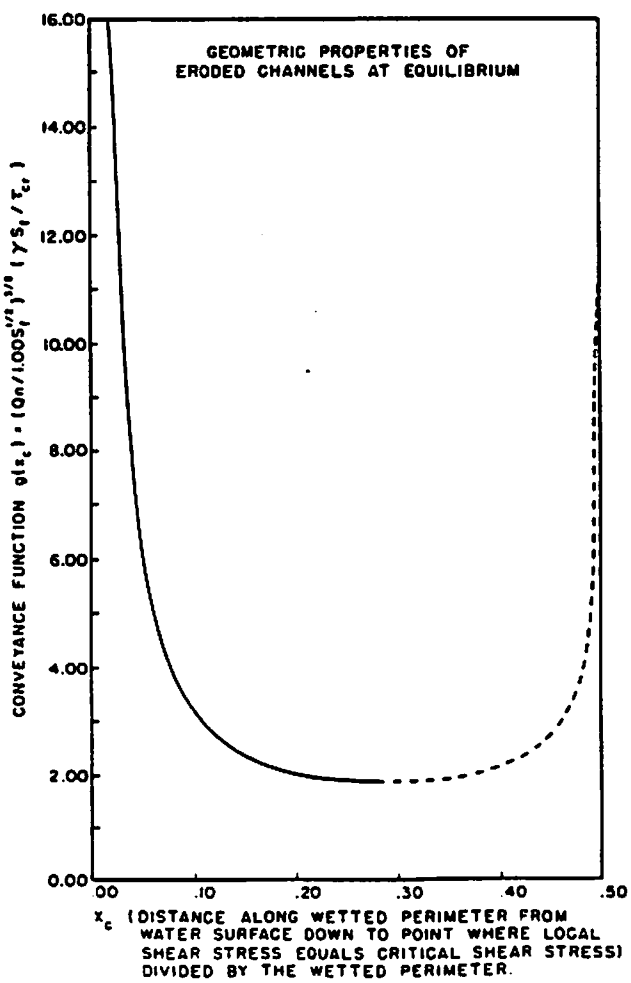

FIG. 4 Function $g(x_c)$ for an eroding channel at equilibrium.

Given a particular value $g(x_c)$, a value of x_c is obtained from Fig. 3. Having determined x_c, a value for $R_* =$ hydraulic radius/wetted perimeter and $W_* =$ width /wetted perimeter is read from Fig. 4. The width of the channel before it reaches the nonerodible layer is then calculated from:

$$W_{ac} = (Qn/S_f^{1/2})^{3/8}\ W_*/R^{5/8}) \quad \text{[12]}$$

The channel moves downward at the rate d_{ch}:

$$d_{ch} = D_c/\rho_{soil} = K_{ch}\ (1.35\tau - \tau_{cr})^{1.05}/\rho_{soil} \quad \text{[13]}$$

where ρ_{soil} = mass density of the soil in place. The erosion rate in the channel is:

$$E_{ch} = W_{ac}\ K_{ch}\ (1.35\ \tau - \tau_{cr})^{1.05}\ t_b \quad \text{[14]}$$

where E_{ch} is the soil loss per unit channel length for the storm (mass/unit length).

Erosion rate e_p (mass/unit area of wetted perimeter/unit time) normal to the wetted perimeter at a point is assumed equal to:

$$e_p = K_{ch}\ (\tau_x - \tau_{cr})^{1.05} \quad \text{[15]}$$

where τ_x = the shear stress at a given point along the wetted perimeter. In order for a channel to be eroding downward in an equilibrium shape at an equilibrium rate, the vertical component of the erosion rates, e_p, must be equal at all points along the wetted perimeter. Equations [10 - 13] and Figs. 3 and 4 are based on this condition. The 1.35 factor is the ratio of the shear stress in the center of the channel to the average shear stress for the cross section.

Once the channel reaches the nonerodible boundary, erosion rate decreases with time as the channel widens. The rate decreases even if discharge rate remains constant. The width W of the channel at any time after the channel has eroded to the nonerodible layer is estimated by:

$$W_* = [1 - \exp(-t_*)] \quad \text{[16]}$$

where:

$$W_* = (W - W_i)/(W_f - W_i) \quad \text{[17]}$$

$$t_* = (t - t_i)\,(dW/dt)_i/(W_f - W_i) \quad [18]$$

where W = width at t, W_i = width at t_i, W_f = final eroded width for $t \to \infty$ and the given Q, t = time, and $(dW/dt)_i$ = rate that channel widens at $t = t_i$. The initial widening rate is given by:

$$(dW/dt)_i = 2K_{ch}\,(\tau_b - \tau_{cr})^{1.05}/\rho_{soil} \quad [19]$$

where τ_b is given by:

$$f(x_b) = \left(\tau_b/\bar{\tau}\right) = \exp\,[0.127 - 0.516 \ln x_b - 0.408 (\ln x_b)^2 - 0.0344 (\ln x_b)^3] \qquad x_b > 0.02 \quad [20]$$

or

$$f(x_b) = \left(\tau_b/\bar{\tau}\right) = 0.13\, x_b/0.02 \qquad x_b < 0.02 \quad [21]$$

where x_b = flow depth/wetted perimeter.

The final width W_f is determined by finding the x_{cf} that gives:

$$(Qn/S_f^{1/2})^{3/8}\,(\gamma S_f/\tau_{cr}) = \left\{[x_{cf}(1 - 2x_{cf})]^{3/8}\, f(x_{cf})\right\}^{-1} \quad [22]$$

where $f(x_{cf})$ is the function given by equation [20] or [21] and evaluated at x_{cf}. The final width is:

$$W_f = \left\{(Qn/S_f^{1/2})\,[(1 - 2x_{cf})/x_{cf}^{5/3}]\right\}^{3/8} \quad [23]$$

Equations [16 - 23] are based on the assumption that in a rectangular channel on a nonerodible layer, the channel widens at the rate that the flow erodes the channel wall at the nonerodible layer. Widening ceases when the shear stress at the nonerodible boundary equals the critical shear stress.

Channel erosion after the channel reaches the nonerodible layer is:

$$E_{ch} = \Delta W\, H_{sw}\rho_{soil} \quad [24]$$

where ΔW = the change in width calculated from equations [16 - 23] and H_{sw} = the height of the channel sidewall.

IMPOUNDMENT ELEMENT

The impoundment element describes deposition behind impoundment terraces and other small structures that drain between storms through a pipe near the bottom of the impoundment where an orifice controls discharge.

Deposition is the main sedimentation process occurring in impoundments. Since transport capacity in impoundments is essentially nonexistent, the amount of sediment trapped in an impoundment depends primarily on time available for sediment to settle to the bottom of the impoundment before flow can carry the particles from the impoundment. The equations for the impoundment element were developed from regression analyses where relationships were fitted to simulate the data from a more complex model (Laflen et al., 1978). That model had previously been validated with field data (Laflen et al., 1972.

The fraction of a given particle type that passes through the impoundment is:

$$F_{pi} = A_p \exp(B_p\, d_{epi}) \quad [25]$$

where F_{pi} = fraction passing through the impoundment for particle type i, A_p and B_p = coefficients given below, and d_{epi} = the equivalent sand diameter in microns of particle tipe i. Equation [25] is integrated over a particle class interval to obtain the total discharge for the particle class.

The coefficients A_p and B_p are given by:

$$A_p = 1.136 \exp(Z_s) \quad [26]$$

$$B_p = -0.152 \exp(Y_s) \quad [27]$$

with Z_s and Y_s in turn given by:

$$Z_s = (-6.68 \times 10^{-6})\, f\, (0.3048)^{B-2} - 0.0903B + (1.19 \times 10^{-4})C_{or} - (1.21 \times 10^{-4})V_{in} - 0.0185I \quad [28]$$

$$Y_s = (3.28 \times 10^{-6})\, f\, (0.3048)^{B-2} + 0.123B - (2.4 \times 10^{-4})C_{or} + (2.86 \times 10^{-4})\, V_{in} - 0.0108I \quad [29]$$

where f and B = coefficient and exponent in the power equation relating surface area to depth $S_a = fY_d^B$, Y_d = depth in the impoundment (m), S_a = surface area (m^2), V_{in} = volume of runoff reaching the impoundment (m^3), and I = infiltration rate in the impoundment (mm/h). The coefficient C_{or} related to the orifice in the pipe outlet is given by:

$$C_{or} = 0.15\, d_{or}^2 \quad [30]$$

where d_{or} = diameter of the orifice (mm).

Less water leaves the impoundment than entered it because of infiltration through the boundary of the impoundment. The volume leaving is estimated by:

$$V_{out} = 0.95\, V_{in} \exp(Z_r) \quad [31]$$

where V_{out} = volume of runoff discharged, and Z_r is given by:

$$Z_r = (-9.29 \times 10^{-6})\, f\, (0.3048)^{B-2} + 0.0282B + (1.25 \times 10^{-4})C_{or} - (1.09 \times 10^{-4})\, V_{in} - 0.0304I \quad [32]$$

In addition:

$$\text{If } I = 0.0,\; V_{out} = V_{in} \quad [33]$$

$$\text{If } V_{out} > V_{in},\; V_{out} = V_{in} \quad [34]$$

are additional constraints on V_{out} from equation [31] because 0 and V_{in} are not lower and upper limits for equations [31] and [32].

ERODED SEDIMENT CHARACTERISTICS

Sediment eroded from field-sized areas is often a mixture of primary particles and aggregates. The size and density distribution of these particles as they are detached is a function of soil properties, soil management, and rainfall and runoff characteristics. If deposition changes the distribution, usually the coarse and dense particles are deposited first, leaving a mixture of finer sediment. The initial particle input to the model is the distribution of the sediment as it is detached; the model calculates a new distribution when it calculates the occurrence of deposition. No selectivity is assumed in detachment of particles.

TABLE 1. TYPICAL SEDIMENT CHARACTERISTICS OF DETACHED SEDIMENT BEFORE DEPOSITION FOR A MIDWESTERN SOIL.*

Particle type	Diameter	Specific gravity	Fraction of total
	mm		mass basis
Primary clay	0.002	2.60	0.05
Primary silt	0.010	2.65	0.08
Small aggregate	0.030	1.80	0.50
Large aggregate	0.500	1.60	0.31
Primary sand	0.200	2.65	0.06

*Particle distribution in soil mass: Clay = 25%, Silt = 60%, Sand = 15%.

Based on a survey of existing data, values given in Table 1 are typical of some midwestern soils. If the particle distribution is unknown, the model estimates the distribution from the primary particle size distribution of the soil mass using the following equations:

$$PSA = SAO\ (1.0 - CLO)^{2.49} \qquad [35]$$

$$PSI = 0.13\ SIO \qquad [36]$$

$$PCL = 0.2\ CLO \qquad [37]$$

$$SAG = 2\ CLO \quad CLO < 0.25 \qquad [38]$$

$$SAG = 0.28\ (CLO - 0.25) + 0.5 \quad 0.25 \leq CLO \leq 0.50 \qquad [39]$$

$$SAG = 0.57 \quad 0.5 < CLO \qquad [40]$$

$$LAG = 1.0 - PSA - PS - PCL - SAG \qquad [41]$$

if LAG < 0.0, multiply PSA, PS, PCL, and SAG by same ratio to make:

$$LAG = 0.0 \qquad [42]$$

The variables, CLO, SIO, SAO, PCL, PSI, PSA, SAG, and LAG, are respectively, fractions for primary clay, silt, and sand in the original soil mass, and primary clay, silt, sand, and small and large aggregates in the sediment at the point of detachment. The diameters for the particles are defined as:

$$DPCL = 0.002\ mm \qquad [43]$$

$$DPSI = 0.010\ mm \qquad [44]$$

$$DPSA = 0.200\ mm \qquad [45]$$

$$DSAG = 0.03\ mm \quad CLO < 0.25 \qquad [46]$$

$$DSAG = 0.20\ (CLO - 0.25) + 0.03\ mm \quad 0.25 \leq CLO \leq 0.60 \qquad [47]$$

$$DSAG = 0.1\ mm \quad 0.60 < CLO \qquad [48]$$

$$DLAG = 2\ CLO\ mm \qquad [49]$$

where DPCL, DPSI, DPSA, DSAG, and DLAG are, respectively, the diameters of the primary clay, silt, and sand, and the small and large aggregates in the sediment. The assumed specific gravities are shown in Table 1. The primary particle composition of the aggregates is estimated from:

$$CLSAG = SAG\ [CLO/(CLO + SIO)] \qquad [50]$$

$$SISAG = SAG\ [SIO/(CLO + SIO)] \qquad [51]$$

$$SASAG = 0.0 \qquad [52]$$

$$CLLAG = CLO - PCL - CLSAG \qquad [53]$$

$$SILAG = SIO - PSI - SISAG \qquad [54]$$

$$SALAG = SAO - PSA \qquad [55]$$

where CLSAG, SISAG, and SASAG = fractions of the total for the sediment of, respectively, primary clay, silt, and sand in the small aggregates in the sediment load, and CLLAG, SILAG, and SALAG are corresponding fractions for the large aggregates.

If the fraction of clay in the large aggregate based on the mass of the large aggregate and not on the total mass of sediment is less than 0.5 times CLO, the distribution of the particle types is recomputed. A sum of Γ is computed whereby:

$$\Gamma = PCL + PSI + PSA \qquad [56]$$

The fractions PSA, PSI, and PCL are not changed. The new SAG is:

$$SAG = (0.3 + 0.5\ \Gamma)\ (CLO + SIO)/([1 - 0.5(CLO + SIO)] \qquad [57]$$

Equation [57] is derived given (i) previously determined values for PCL, PSI, and PSA; (ii) the assumption that the sum of primary clay fractions for the total sediment is 1; and (iii) the assumption that the fraction of primary clay in LAG equals one half of the primary clay in the original soil.

The model also computes an enrichment ratio using values for specific surface area of organic matter, clay, silt, and sand. Organic matter is distributed among the particle types based on the proportion of primary clay in each type. The enrichment ratio is the ratio of total specific surface area of the sediment to that for the original soil.

DISCUSSION

The model gave reasonable results, when compared with data from concave plots under simulated rainfall, single terrace watersheds, small watersheds with impoundment terraces, and a small watershed under conservation tillage. The simulations were made using measured rainfall and runoff values.

Concave Plots

Three concave plots 10.7 m long were carefully shaped in uniform soil so that slope along the plots continuously decreased from 18 percent at the upper end to 0 percent at the lower end (Foster et al., 1980b). Simulated rainfall at 64 mm/h was applied to one of the plots and deposi-

TABLE 2. COMPARISON OF OBSERVED SOIL LOSS FROM CONCAVE FIELD PLOTS WITH THAT COMPUTED BY THE MODEL.

	Plot length	Slope at lower end	Sediment yield	Particle distribution in size class				
				0.002	0.03	0.3	0.75	1.5 mm
	m	%	kg/m	Fraction				
Observed*	7.0	6	8.6	0.05	0.36	0.15	0.17	0.27
Observed	8.8	3	3.9	0.07	0.48	0.12	0.12	0.21
Computed			6.5	0.08	0.58	0.24	0.10	0.01
Observed	10.7	0	3.0	0.10	0.85	0.02	0.01	0.02
Computed			3.0	0.19	0.80	0.01	0.00	0.00

*These data were used to calibrate soil erodibility factor, Manning's n, and particle distribution of sediment reaching deposition area. Source of data: Foster et al. (1980b).

tion began at 7 m from the upper end. Plot ends were installed at 7.0 m and 8.8 m on the other two plots. The measured particle distribution of the sediment entering the deposition area was used, and the soil erodibility factor and Manning's n were adjusted in the model to give the observed soil loss and particle distribution for the 7.0 m plot. The results shown in Table 2 for the 8.8 and 10.7 m plots were obtained using these calibrated values and the approximate slope shape curves in the model rather than the actual slope shape.

Single Terrace Watersheds

Soil loss was simulated for eight years of data, about 53 runoff producing storms, from small, single terrace watersheds at Guthrie, Oklahoma (Daniel et al., 1943). The simulations were made without calibration using instructions in the user manual for the model (Foster et al., 1980a). Table 3 gives computed and measured results.

Impoundment Terraces

Soil loss was simulated under a range of rainfall and runoff characteristics for six selected storms at the Charles City, and Guthrie Center, Iowa, and for five storms at Eldora, Iowa. Data were taken from an impoundment terrace study (Laflen et al., 1972). The model was run using the user manual instruction without calibration. Table 4 gives the results.

Small Watershed

Simulations were run without calibrating for approximately 2½ years of data, about 35 runoff producing storms, from the P2 watershed at Watkinsville, Georgia in conservation tillage systems for corn (Smith et al., 1978). Deposition in the backwater from the flume at the watershed outlet was modeled. Deposition measured in the flume backwater was about equal to the measured sediment yield on a similar, nearby watershed (Langdale et al., 1979). The computed sediment yield total for the period of record was 1.47 kg/m², while the measured value was 1.95 kg/m².

TABLE 3. COMPUTED AND OBSERVED SOIL LOSS FOR 8 YEARS OF DATA FROM SINGLE TERRACE WATERSHEDS AT GUTHRIE, OKLAHOMA*.

Terrace	Total soil loss for period per unit area of watershed	
	Observed	Computed
	kg/m²	kg/m²
Uniform grade of 0.0017, 457 m long	4.8	4.6
Uniform grade of 0.005, 457 m long	12.1	10.6
Variable grade, 0.005 at outlet to 0 at upper end, 871 m long	13.8	11.9
Variable grade, 0.0033 at outlet to 0 at upper end, 773 m long	12.2	6.4

*Source of data: Daniel et al. (1943)

Overland Flow Detachment

The relationships for detachment used in the overland flow element gave good results for a watershed at Treynor, Iowa. Estimates were better than those from the USLE using storm EI (Foster et al., 1977) and those obtained using the USLE and runoff volume and peak discharge (Onstad et al., 1977) as measures of erosivity. These results were confirmed by Lombardi (1979) for data from natural rainfall on uniform slopes. On long-term simulation, the model should produce results similar to those of the USLE for uniform slopes.

Overland Flow Sediment Transport

As the results in Table 2 indicate, estimates of sediment transport by overland flow may be in error by a factor of two. The Yalin equation was selected to describe sediment transport by overland flow after studies showed that it gave better results than did several other widely used equations (Alonso, 1980; Neibling and Foster, 1980). However, overland flow conditions are outside the range of most sediment transport equations developed for stream flow. Many give results greatly in error for overland flow.

Channel Detachment

The relationships for channel erosion are the ones most likely to be in error, because data for flow concentrations 300 mm wide from the studies (Meyer et al., 1975; Lane and Foster, 1980) where the relationships were derived may not apply to 2 m wide channels. Also, parameter values for channel soil erodibility and critical shear stress are not readily available. Few models except that of Bruce et al. (1975) consider the decay in erosion with time due to previous erosion. This component of the model may require calibration.

TABLE 4. SIMULATED AND OBSERVED SOIL LOSS FOR IMPOUNDMENT TERRACES IN IOWA.

Location	Total soil loss per unit area of watershed for selected storms	
	Observed	Computed
	kg/m²	kg/m²
Eldora	0.115	0.069
Charles City	0.043	0.016
Guthrie Center	0.050	0.050

SUMMARY

An erosion-sediment yield model for field-sized areas was developed for use on a storm-by-storm basis. The overall objective was to develop a model incorporating fundamental erosion-sediment transport relationships for use in evaluating best management practices for control of erosion and sediment yield from farm fields. The procedure allows parameters to change along the overland flow profile and along waterways to represent both spatial variability and the variations that occur from storm-to-storm. Many of the model parameters are directly from the Universal Soil-Loss Equation (USLE) and other similar, process-type relationships. For this reason, we feel that the model has immediate applications without extensive calibration.

Individual components of the model were tested using experimental data from studies of overland flow, erodible channels, and impoundments. Testing suggests that the model gives reasonable results and may be a useful tool for analyzing the influence of alternate management practices on erosion and sediment yield from field-sized-areas.

References

1 Alonso, C. V. 1980. Selecting a formula to estimate sediment transport in nonvegetated channels. In: CREAMS - A Field Scale Model for Chemicals, Runoff, and Erosion from Agricultural Management Systems. Vol III: Supporting Documentation. Conservation Research Report No. 26. USDA, Sci. and Educ. Admin. Chpt. 5. pp. 426-439.

2 Beasley, D. B., E. J. Monke, and L. F. Huggins. 1980. ANSWERS: A model for watershed planning. TRANSACTIONS of the ASAE. 23(4):839-944.

3 Bruce, R. R., L. A. Harper, R. A. Leonard, W. M. Snyder, and A. W. Thomas. 1975. A model for runoff of pesticides from small upland watersheds. J. Environ. Qual. 4(4):541-548.

4 Chow, V. T. 1959. Open-Channel Hydraulics. McGraw-Hill Book Co. New York, NY. 680 pp.

5 Davis, S. S. 1978. Deposition of nonuniform sediment by overland flow on concave slopes. M. S. Thesis. Purdue Univ., W. Lafayette, IN.

6 Daniel, H. A., H. M. Elwell and M. B. Cox. 1943. Investigations in erosion control and reclamation of eroded land at the Red Plains Conservation Experiment Station, Guthrie, OK, 1930-40. USDA-Tech. Bull. No. 837. 94 pp.

7 Donigian, A. S., Jr. and N. H. Crawford. 1976. Modeling nonpoint source pollution from the land surface. EPA-600/3-76-083. U. S. Environ. Protection Agency. 279 pp.

8 Einstein, H. A. 1968. Deposition of suspended particles in a gravel bed. J. Hydr. Div. ASCE. 94(HY5):1197-1205.

9 Ellison, W. D. 1947. Soil erosion studies. AGRICULTURAL ENGINEERING 28:145-146, 127-201, 245-248, 297-300, 349-351, 402-405, 442-444.

10 Foster, G. R., L. J. Lane, and J. D. Nowlin. 1980a. A model to estimate sediment yield from field sized areas: Selection of parameter values: In: CREAMS - A Field Scale Model for Chemicals, Runoff, and Erosion from Agricultural Management Systems. Vol. II: User Manual. Conservation Research Report No. 26. USDA, Sci. and Educ. Admin. Chpt. 2. pp. 193-281.

11 Foster, G. R., W. H. Neibling, S. S. Davis, and E. E. Alberts. 1980b. Modeling particle segregation during deposition by overland flow. In: Proc. Hydrologic Transport Modeling Symposium. ASAE Publ. 4-80. pp. 184-195.

12 Foster, G. R. and L. D. Meyer. 1972. Transport of soil particles by shallow flow. TRANSACTIONS of the ASAE 15(1):99-102.

13 Foster, G. R. and L. D. Meyer. 1975. Mathematical simulation of upland erosion by fundamental erosion mechanics. In: Present and Prospective Technology for Predicting Sediment Yields and Sources. ARS-S-40. USDA, Agric. Research Ser. pp. 190-207.

14 Foster, G. R., L. D. Meyer, and C. A. Onstad. 1977. A runoff erosivity factor and variable slope length exponents for soil loss estimates. TRANSACTIONS of the ASAE 20(4):683-687.

15 Graf, W. H. 1971. Hydraulics of Sediment Transport. McGraw-Hill Book Co. New York, NY. 544 pp.

16 Khaleel, R., G. R. Foster, K. R. Reddy, M. R. Overcash and P. W. Westerman. 1979. A nonpoint source model for land areas receiving animal wastes: III. A conceptual model for sediment and manure transport. TRANSACTIONS of the ASAE 22(5):1353-1361.

17 Laflen, J. M., H. P. Johnson, and R. O. Hartwig. 1978. Sedimentation modeling of impoundment terraces. TRANSACTIONS of the ASAE 21(6):1131-1135.

18 Laflen, J. M., H. P. Johnson, and R. C. Reeves. 1972. Soil loss from tile outlet terraces. J. Soil and Water Conserv. 27(2):74-77.

19 Lane, L. J. and G. R. Foster. 1980. Concentrated flow relationships. In: CREAMS - A Field Scale Model for Chemicals, Runoff, and Erosion from Agricultural Management Systems. Vol. III: Supporting Documentation. Conservation Research Report No. 26. USDA, Sci. and Educ. Admin. Chpt. 10. pp. 474-485.

20 Lane, L. J., D. A. Woolhiser, and V. Yevjevich. 1975. Influence of simplification in watershed geometry in simulation of surface runoff. Hydrology Paper No. 81. Colorado State Univ., Fort Collins. 50 pp.

21 Langdale, G. W., A. P. Barnett, R. A. Leonard, and W. G. Fleming. 1979. Reduction of soil erosion by no-till systems in the Southern Piedmont. TRANSACTIONS of the ASAE 22(1):82-86, 92.

22 Li, R. M. 1977. Water and sediment routing from watersheds. In: Proc. River Mechanics Institute. Colorado State Univ., Fort Collins. Chpt. 9.

23 Lombardi, F. 1979. Universal Soil Loss Equation (USLE), runoff erosivity factor, slope length exponent, and slope steepness exponent for individual storms. Ph.D. Thesis. Purdue Univ., W. Lafayette, IN. 128 pp.

24 Meyer, L. D., G. R. Foster, and S. Nikolov. 1975. Effect of flow rate and canopy on rill erosion. TRANSACTIONS of the ASAE 18(5):905-911.

25 Meyer, L. D. and W. H. Wischmeier. 1969. Mathematical simulation of the process of soil erosion by water. TRANSACTIONS of the ASAE12(6):754-758, 762.

26 Neibling, W. H. and G. R. Foster. 1980. Sediment transport capacity of overland flow. In: CREAMS - A Field Scale Model for Chemicals, Runoff, and Erosion from Agricultural Management Systems. Vol. III: Supporting Documentation. Conservation Research Report No. 26. USDA, Sci. and Educ. Admin. Chpt. 10. pp. 463-473.

27 Onstad, C. A., R. F. Piest, and K. E. Saxton. 1976. Watershed erosion model validation for Southwest Iowa. In: Proc. of the Third Federal Inter-Agency Sedimentation Confer. Water Resources Council. Washington, DC. Chpt. 1. pp. 23-24.

28 Smith, C. N., R. A. Leonard, G. W. Langdale, and G. W. Bailey. 1978. Transport of agricultural chemicals from small upland Piedmont watersheds. EPA-600/3-78-056. U. S. Environ. Protection Agency. 364 pp.

29 U. S. Department of Agriculture (USDA), 1980. CREAMS - A Field Scale Model for Chemicals, Runoff, and Erosion from Agricultural Management Systems. Conservation Research Report No. 26. Sci. and Educ. Admin. 643 pp.

30 Williams, J. R. 1975. Sediment-yield prediction with universal equation using runoff energy factor. In: Present and Prospective Technology for Predicting Sediment Yields and Sources. ARS-S-40. USDA, Agric. Research Ser. pp. 244-253.

31 Wischmeier, W. H. and D. D. Smith. 1978. Predicting Rainfall Erosion Losses. Agricultural Handbook No. 537. USDA, Sci. and Educ. Admin. 58 pp.

32 Yalin, Y. S. 1963. An expression for bed-load transportation. J. Hydr. Div. ASCE. 89(HY3):221-250.

LIST OF SYMBOLS

A_p	Coefficient in equation for deposition in an impoundment
B	Exponent in surface area - depth relationship for an impoundment
B_p	Exponent in equation for deposition in an impoundment
CLLAG	Clay content of large aggregates, fraction of total sediment
CLO	Fraction of original soil made up of primary clay
CLSAG	Clay content of small aggregates, fraction of total sediment
C_o	Orifice coefficient for drainage from impoundment
d_c	Rate that channel erodes downward, (depth/time)
d_{eq}	Equivalent sand diameter of a sediment particle
d_o	Diameter of orifice in an impoundment drain
D_c	Rate of sediment detachment by flow in channels (mass/area/time)
D_d	Rate of deposition by flow (mass/area/time)
D_f	Rate of detachment or deposition by flow (mass/area/time)
D_r	Rate of sediment detachment by rill erosion, (mass/area/time)

D_l	Rate of detachment by flow at lower end of a segment, (mass/area/time)
D_L	Rate of lateral inflow of sediment, (mass/area or length/time)
D_{Li}	Rate of sediment from interrill areas (mass/area/time)
D_u	Rate of detachment by flow at upper end of a segment, (mass/area/time)
DLAG	Diameter of large aggregate sediment particles
DPCL	Diameter of primary clay sediment particles
DPSA	Diameter of primary sand sediment particles
DPSI	Diameter of primary silt sediment particles
DSAG	Diameter of small aggregate sediment particles
E_r	Erosion rate normal to channel boundary, (mass/area/time)
E_{ch}	Erosion rate per unit length of channel, (mass/length of channel)
EI	Rainfall erosivity, total storm energy times maximum 30-min intensity
f	Coefficient in surface area-depth relationship for impoundment
$f(x_*)$	Shear stress distribution around a channel
F_{pi}	Fraction of a particular particle class deposited in an impoundment
$g(x_e)$	Conveyance function for flow in an eroding channel at equilibrium
H_{sw}	Height of channel sidewall
i	Particle class index
I	Infiltration rate through boundary of an impoundment
K	Soil erodibility factor for the USLE
K_{ch}	Soil erodibility factor for channel erosion
LAG	Fraction of sediment made up of large aggregates
n	Manning's n
n_{bar}	Manning's n for bare, smooth, overland flow surface
n_{cov}	Manning's n for a covered or rough overland flow surface
P	Contouring component of USLE supporting practices factor
PCL	Fraction of sediment made up of primary clay
PSA	Fraction of sediment made up of primary sand
PSI	Fraction of sediment made up of primary silt
q_s	Sediment load, (mass/width/time)
q_{su}	Sediment load at upper end of segment, (mass/width/time)
q_w	Rate of runoff discharge per unit width (volume/time/width)
Q	Discharge rate, (volume/time)
R_*	Ratio of hydraulic radius to wetted perimeter
s_o	Sine of angle of slope
S_a	Surface area in an impoundment
S_f	Friction slope for flow hydraulics in a channel
SAG	Fraction of sediment made up of small aggregates
SALAG	Fraction of sand in large aggregates, fraction of total sediment
SAO	Fraction of original soil made up of primary sand
SASAG	Fraction of sand in small aggregates, fraction of total sediment
SILAG	Fraction of silt in large aggregates, fraction of total sediment
SIO	Fraction of original soil made up of primary silt
SISAG	Fraction of silt in small aggregates, fraction of total sediment
t	Time
t_b	Time that shear stress exceeds critical shear stress
t_*	Normalized time for channel erosion
t_i	Initial time
T_c	Transport capacity, (mass/area/time)
V_{in}	Runoff volume into impounment
V_{out}	Runoff volume out of impoundment
V_s	Particle fall velocity
V_u	Runoff volume per unit area, (depth)
W	Channel width
W_*	Normalized channel width
W_{eq}	Width of an eroding channel at equilibrium
W_f	Final eroded channel width
W_i	Initial channel width
x	Distance
x_b	Normalized distance around wetted perimeter to nonerodible boundary
x_e	Normalized distance around wetted perimeter to location where $\tau=\tau_{cr}$ for an eroding channel at equilibrium
x_c	Normalized distance around wetted perimeter to location where $\tau=\tau_{cr}$ at nonerodible boundary
y	Flow depth
Y_d	Depth in impoundment
Y_e	Exponent in deposition equation for an impoundment
Z_r	Exponent in equation for runoff reduction by an impoundment.
Z_e	Exponent in equation for deposition in impoundment
α	Reaction coefficient for deposition by flow, $length^{-1}$
γ	Weight density of water
Γ	Sum of PCL, PSI, and PSA
Δx	Segment length
ΔW	Change in channel width
η	Slope length exponent for rill erosion
ε	Coefficient in deposition equation
ρ_{soil}	Mass density of soil in place
σ_p	Peak runoff rate, (depth/time)
$\bar{\tau}$	Average shear stress around wetted perimeter
τ_b	Shear stress in channel at a nonerodible boundary
τ_{cr}	Critical shear stress
τ_{soil}	Shear stress acting on soil
τ_a	The shear stress at a given point along the wetted perimeter.
Φ	Soil loss ratio from USLE